

Isovector unpolarized quark distribution in the nucleon in the large- N_c limit

P.V. Pobylitsa, M.V. Polyakov

Petersburg Nuclear Physics Institute, Gatchina, St. Petersburg 188350, Russia

K. Goeke, T. Watabe, and C. Weiss

*Institut für Theoretische Physik II, Ruhr-Universität Bochum,
D-44780 Bochum, Germany*

Abstract

We calculate the isovector (flavor-nonsinglet) unpolarized quark- and antiquark distributions in the nucleon at a low normalization point in the large- N_c limit. The nucleon is described as a soliton of the effective chiral theory. The isovector distribution appears in the next-to-leading order of the $1/N_c$ -expansion. Numerical results for the quark- and antiquark distributions compare well with the parametrizations of the data at a low normalization point. This large- N_c approach gives a flavor asymmetry of the antiquark distribution (violation of the Gottfried sum rule) in good agreement with the measurements.

PACS: 13.60.Hb, 14.20.Dh, 12.38.Lg, 12.39.Ki, 11.15.Pg

Keywords: parton distributions at low q^2 , unpolarized structure functions, Gottfried sum rule, large N_c limit, chiral soliton model of the nucleon

Contents

1	Introduction	3
2	The nucleon as a chiral soliton	5
3	The isovector unpolarized quark distribution	8
3.1	The isovector distribution function in the large- N_c limit	8
3.2	Ultraviolet regularization	14
3.3	The isospin sum rule	15
3.4	The Gottfried sum	16
4	Numerical results and discussion	17
5	Conclusions	20
A	Evaluation of the isovector distribution	21

1 Introduction

The parton distribution functions of the nucleon contain the non-perturbative information which enters in the cross section for deep-inelastic scattering and a variety of other hard processes. Their scale dependence in the asymptotic region is governed by perturbative QCD and well understood. The starting points of the perturbative evolution, however, that is, the distributions at a relatively low normalization point, belong to the domain of non-perturbative physics and can at present only be estimated using approximate methods to deal with the problem of the structure of the nucleon.

A very useful approximation is the theoretical limit of a large number of colors, $N_c \rightarrow \infty$. It is known that in this limit QCD becomes equivalent to an effective theory of mesons, with baryons emerging as solitonic excitations [1]. At low energies the structure of the effective theory is determined by the spontaneous breaking of chiral symmetry. The first realization of the idea of the nucleon as a soliton of the pion field was proposed by Skyrme [2, 3], which was, however, based on an arbitrary choice of higher-derivative terms of chiral Lagrangian. A more realistic effective action for the pion field is given by the integral over quark fields with a dynamically generated mass, interacting with the pion field in a minimal chirally invariant way [4]. Such an effective action has been derived from the instanton vacuum of QCD, which provides a microscopic mechanism for the dynamical breaking of chiral symmetry [5]. The chiral quark-soliton model of the nucleon based on this effective action [6, 7] has been very successful in describing hadronic observables such as the nucleon mass, $N\Delta$ -splitting, electromagnetic and weak form factors *etc.* [8].

Recently it has been demonstrated that it is possible to compute also the leading-twist parton distributions at a low normalization point in the chiral quark-soliton model of the nucleon [9, 10, 11]. This field-theoretic description of the nucleon allows to preserve all general requirements on parton distributions, such as positivity and the partonic sum rules which hold in QCD. In particular, it allows a consistent calculation of the antiquark distributions. The approach has by now been extended to transverse polarized distributions [12] as well as to off-forward quark distributions [13].

The large- N_c limit implies a classification of the parton distribution functions in “large” and “small” ones [9]. Generally, at large N_c the quark distributions are concentrated at values of $x \sim 1/N_c$, and with the chiral quark-soliton model we aim to compute them for values of x of this parametric order. The distribution functions which appear in the leading order of the $1/N_c$ -expansion are of the form

$$D^{\text{large}}(x) \sim N_c^2 \rho(N_c x), \quad (1.1)$$

where $\rho(y)$ is a stable function in the large N_c -limit, which depends on the particular distribution considered. They are the isosinglet unpolarized and isovector (longitudinally or transverse polarized) distributions, which have been computed in Refs.[9, 10, 12]. The isovector unpolarized and isosinglet polarized distributions, on the other hand, appear only in the next-to-leading order of the $1/N_c$ -expansion and are of the form

$$D^{\text{small}}(x) \sim N_c \rho(N_c x). \quad (1.2)$$

In this paper we compute the isovector unpolarized quark- and antiquark distributions in the chiral quark-soliton model. The general method for calculating the $1/N_c$ -subleading distributions and a discussion of their properties have been given in Ref.[9]. Here we actually compute the distribution function, including the Gottfried sum, which is a measure of the flavor asymmetry of the antiquark distribution at the low scale [14, 15]. This task requires, among other things, to generalize the analytical and numerical methods for the computation of distribution functions [10] to the case of the $1/N_c$ -subleading distributions, taking into account the rotation of the chiral soliton.

The isovector distribution considered here is of particular interest for understanding the relation of the low-scale parton distributions to the chiral effective dynamics. The distribution functions computed within the effective chiral theory correspond to distributions of “constituent” quarks and antiquarks, *i.e.*, objects which possess a structure in terms of QCD quarks and gluon¹ [9]. The parameter governing the compositeness of the constituent quark is the ratio of the dynamical quark mass to the ultraviolet cutoff of the effective theory — the “size” of the constituent quark. In the instanton vacuum this ratio is proportional to the small packing fraction of instantons, $(\bar{\rho}/R)^2$. Before comparing the quark- and antiquark distributions computed in the effective chiral theory with the parametrizations of the data at a low normalization point [18] one should “resolve” the structure of the constituent quark. From the singlet distribution, $u(x) + d(x) + \bar{u}(x) + \bar{d}(x)$, “resolving” the constituent quark structure one recovers the true singlet quark and gluon distributions. Phenomenologically one finds that gluons carry about 30% of the nucleon momentum at a normalization point of $\mu \approx 600$ MeV, so in the singlet case the “resolution” of the constituent quark structure is a rather sizable effect [9, 10]. In the isovector case considered here the change of the distribution due to the “resolution” of the constituent quark structure is expected to be less important, as this distribution does not mix with the gluon distribution and its normalization is scale independent (isospin sum rule). Consequently, the isovector distribution calculated in the effective chiral theory can almost directly be compared with the parametrizations of Ref.[18], allowing one to draw conclusions about the model dynamics even in the absence of a complete understanding of the structure of the constituent quark.

The plan of this paper is as follows. Section 2 contains a brief exposition of the effective chiral theory and the description of the nucleon as a chiral soliton, including the semiclassical quantization procedure. In Section 3 we derive the expressions for the isovector quark distribution functions in the effective chiral theory and discuss their properties. We first outline the expansion in the soliton angular velocity ($1/N_c$ -expansion) which is necessary for computing the “small” ($1/N_c$ -suppressed) distribution functions, in particular the isovector unpolarized one. We then discuss the important issue of ultraviolet regularization, which has been treated in detail in Ref.[10]. We show that the distributions obtained in our approach satisfy the isospin sum rule. We also discuss the Gottfried sum. In Section 4 we briefly describe the numerical technique used for computation of the “small” $1/N_c$ -suppressed distribution functions. Similarly to the “large” $1/N_c$ -leading distributions they are computed as sums over quark single-particle levels in the background pion field; however, now one is dealing with double sums over levels. We then discuss the numerical results and compare

¹For a more detailed discussion of this complex issue we refer to Refs.[16, 17]; see also Ref.[11].

them to the parametrizations of the data at a low normalization point [18]. Conclusions and an outlook are given in Section 5.

A calculation of the isovector unpolarized and isosinglet polarized distributions following the approach of Refs.[9, 10] has recently been performed by Wakamatsu and Kubota [19]. However, these authors have neglected certain contributions to the distribution function, which are important in particular at small values of x , as we shall discuss below. Also, a calculation of the isovector unpolarized structure function in a related approach has been reported in Ref.[20]. In that calculation, however, only the contribution of the so-called valence level is taken into account. This approximation leads to a number of inconsistencies, as has been discussed in Refs.[9, 10].

2 The nucleon as a chiral soliton

The starting point for the chiral quark–soliton model of the nucleon is the effective action for the pion field, which is obtained by integrating over quark fields in the background pion field [4, 5],

$$\exp(iS_{\text{eff}}[U(x)]) = \int D\psi D\bar{\psi} \exp\left[i \int d^4x \bar{\psi}(i\rlap{\not{\partial}} - MU^{\gamma_5})\psi\right]. \quad (2.1)$$

Here, ψ is the fermion field, M the dynamical quark mass, which is due to the spontaneous breaking of chiral symmetry, and the pion (Goldstone boson) field is described by an $SU(2)$ matrix, $U(x)$, with

$$U^{\gamma_5}(x) = \frac{1 + \gamma_5}{2}U(x) + \frac{1 - \gamma_5}{2}U^\dagger(x). \quad (2.2)$$

In the long-wavelength limit, expanding in derivatives of the pion field, the effective action Eq.(2.1) reproduces the Gasser–Leutwyler Lagrangian with correct coefficients, including the Wess–Zumino term. It is understood that the effective theory defined by Eq.(2.1) is valid for momenta up to an UV cutoff, which is the scale at which the dynamical quark mass drops to zero. We shall take in the discussion here the quark mass to be momentum-independent and assume divergent quantities to be made finite by applying some UV regularization later. [Why this is generally justified will be discussed below.]

The effective action Eq.(2.1) has been derived from the instanton vacuum, which provides a natural mechanism of dynamical chiral symmetry breaking and enables one to express the parameters entering in Eq.(2.1) — the dynamical mass, M , and the ultraviolet cutoff — in terms of the QCD scale parameter, Λ_{QCD} [5]. In particular, the cutoff is given by the average instanton size, $\bar{\rho}^{-1} \simeq 600 \text{ MeV}$

In the effective chiral theory defined by Eq.(2.1) the nucleon is in the large- N_c limit characterized by a classical pion field (“soliton”). In the nucleon rest frame it is of “hedgehog” form [6],

$$\begin{aligned} U_c(\mathbf{x}) &= \exp[i(\mathbf{n} \cdot \boldsymbol{\tau})P(r)], \\ r &= |\mathbf{x}|, \quad \mathbf{n} = \frac{\mathbf{x}}{r}, \end{aligned} \quad (2.3)$$

where $P(r)$ is called the profile function, with $P(0) = -\pi$ and $P(r) \rightarrow 0$ for $r \rightarrow \infty$. Quarks are described by one-particle wave functions, which are determined as the solutions of the Dirac equation in the background pion field,

$$H(U_c)|n\rangle = E_n|n\rangle. \quad (2.4)$$

Here $H(U_c)$ is the single-particle Dirac Hamiltonian in the background pion field given by Eq.(2.3),

$$H(U) = -i\gamma^0\gamma^k\partial_k + M\gamma^0U\gamma^5. \quad (2.5)$$

The spectrum of $H(U_c)$ includes a discrete bound-state level, whose energy is denoted by E_{lev} , as well as the positive and negative Dirac continuum, polarized by the presence of the pion field. The soliton profile, $P(r)$, is determined by minimizing the static energy of the pion field, which is given by the sum of the energy of the bound-state level and the aggregate energy of the negative Dirac continuum, the energy of the free Dirac continuum ($U = 1$) subtracted [6],

$$\begin{aligned} E_{\text{tot}} &= N_c \left[\sum_{\substack{n \\ \text{occup.}}} E_n - \sum_{\substack{n \\ \text{occup.}}} E_n^{(0)} \right] \\ &= N_c E_{\text{lev}} + N_c \sum_{\substack{n \\ \text{neg. cont.}}} (E_n - E_n^{(0)}), \end{aligned} \quad (2.6)$$

and in the leading order of the $1/N_c$ -expansion the nucleon mass is given simply by the value of the energy at the minimum,

$$M_N = E_{\text{tot}} \Big|_{U=U_c}. \quad (2.7)$$

The expression for the energy of the pion field, Eq.(2.6), contains a logarithmic ultraviolet divergence due to the contribution of the Dirac continuum and requires regularization. In the calculation of the parton distributions below we shall use a Pauli-Villars regularization (see Subsection 3.2), so we regularize also the energy using the Pauli-Villars method. Following Ref.[11] we define

$$E_{\text{tot,reg}} = N_c E_{\text{lev}} + N_c \left[\sum_{\substack{n \\ \text{neg. cont.}}} (E_n - E_n^{(0)}) - \frac{M^2}{M_{PV}^2} \sum_{\substack{n \\ \text{neg. cont.}}} (E_{PV,n} - E_{PV,n}^{(0)}) \right], \quad (2.8)$$

where $E_{PV,n}$ are the eigenvalues of the Hamiltonian, Eq.(2.5), with M replaced by a regulator mass, M_{PV} , and the same pion field. The value of the regulator mass, which now plays the role of the physical cutoff, can be fixed from the pion decay constant,

$$F_\pi^2 = \frac{N_c M^2}{4\pi^2} \log \frac{M_{PV}^2}{M^2}. \quad (2.9)$$

[Numerically, $F_\pi = 93 \text{ MeV}$.] Note that we do not subtract the finite contribution of the discrete level for the spectrum with the Pauli–Villars mass; this prescription leads to a stable minimum of the regularized energy functional, Eq.(2.8), with respect to the profile function [11]. The soliton profile (the “self-consistent” pion field) for this UV regularization has been determined in Refs.[11, 21].

In higher order of the $1/N_c$ -expansion one must take into account the quantum fluctuations about the saddle-point pion field. A special role play the zero modes of the pion field. In fact, the minimum of the energy, Eq.(2.6), is degenerate with respect to translations of the soliton field in space and to rotations in ordinary and isospin space. For the hedgehog field, Eq.(2.3), the two rotations are equivalent. Quantizing the zero modes, *i.e.*, integrating over collective rotations and translations, gives rise to nucleon states with definite momentum and spin/isospin quantum numbers [3, 6]. One performs a (time-dependent) rotation of the hedgehog field, Eq.(2.3),

$$U_c(\mathbf{x}) \rightarrow R(t) U_c(\mathbf{x}) R^\dagger(t), \quad (2.10)$$

where the collective coordinate, $R(t)$, is a rotation matrix in $SU(2)$ -flavor space. The functional integral over the collective coordinate can be computed systematically within the $1/N_c$ -expansion. The moment of inertia of the soliton is $O(N_c)$ (the nucleon is “heavy”), hence the angular velocity is

$$\Omega \equiv \Omega_a \frac{\tau^a}{2} = -iR^\dagger \dot{R} = O\left(\frac{1}{N_c}\right) \quad (2.11)$$

(the collective motion is “slow”), and one can expand in powers of the angular velocity. To leading order in Ω the collective motion is described by a Hamiltonian

$$H_{\text{rot}} = \frac{S_a^2}{2I} = \frac{T_a^2}{2I}, \quad (2.12)$$

where S_a and T_a are the right and left angular momenta, and the Hamiltonian Eq.(2.12) has been obtained by the “quantization rule”

$$\Omega_a \rightarrow \frac{S_a}{I}. \quad (2.13)$$

Here I denotes the moment of inertia of the soliton. It can be expressed as a double sum over quark single-particle levels in the background pion field,

$$I = \frac{N_c}{6} \sum_{\substack{n \\ \text{occup.}}} \sum_{\substack{m \\ \text{non-occup.}}} \frac{\langle n | \tau^a | m \rangle \langle m | \tau^a | n \rangle}{E_m - E_n}. \quad (2.14)$$

Here the sum over n runs over all occupied states, *i.e.*, the discrete level and the negative Dirac continuum, the sum over m over all non-occupied states, *i.e.*, the positive Dirac continuum.

The Hamiltonian Eq.(2.12) describes a spherical top in spin/isospin space, subject to the constraint $S^2 = T^2$, which is a consequence of the “hedgehog” symmetry of the static pion

field, Eq.(2.3). Its eigenfunctions, classified by $S^2 = T^2$, S_3 and T_3 are given by the Wigner finite-rotation matrices [6],

$$\phi_{S_3 T_3}^{S=T}(R) = \sqrt{2S+1}(-1)^{T+T_3} D_{-T_3, S_3}^{S=T}(R). \quad (2.15)$$

The four nucleon states have $S = T = 1/2$, with $S_3, T_3 = \pm 1/2$, while for $S = T = 3/2$ one obtains the 16 states of the Δ resonance. The rotational energy, $S(S+1)/(2I)$, gives a $1/N_c$ -correction to the nucleon mass, which should be added to Eq.(2.7). In particular, the nucleon- Δ mass splitting is given by

$$M_\Delta - M_N = \frac{3}{2I}. \quad (2.16)$$

The expression for the moment of inertia, Eq.(2.14), contains an ultraviolet divergence which is to be removed by the ultraviolet cutoff. The ultraviolet regularization of the moment of inertia must be consistent with that of the isovector quark distribution function; it will be discussed below in Subsection 3.2.

3 The isovector unpolarized quark distribution

3.1 The isovector distribution function in the large- N_c limit

To compute the twist-2 quark and antiquark distribution functions in the effective chiral theory we start from their “field-theoretic” definition as forward matrix elements of certain light-ray operators in the nucleon, which can be regarded as generating functions for the local twist-2 operators [22]. Alternatively, one could start from the “parton model” definition as numbers of particles carrying a given fraction of the nucleon momentum in the infinite-momentum frame [23] — both ways lead to identical expressions for the quark distribution functions in the chiral quark-soliton model [9, 10]. The unpolarized distribution (f denotes the quark flavor) is given by

$$\begin{aligned} D_{\text{unpol},f}(x) &= \frac{1}{4\pi} \int_{-\infty}^{\infty} dz^- e^{ixp^+ z^-} \langle P | \bar{\psi}_f(0) \gamma^+ \psi_f(z) | P \rangle \Big|_{z^+=0, z_\perp=0}, \\ \bar{D}_{\text{unpol},f}(x) &= -\{x \rightarrow -x\}. \end{aligned} \quad (3.1)$$

Here, z^\pm and γ^\pm denote the usual light-like vector components and Dirac matrices,

$$z^\pm = \frac{z^0 \pm z^3}{\sqrt{2}}, \quad \gamma^\pm = \frac{\gamma^0 \pm \gamma^3}{\sqrt{2}}. \quad (3.2)$$

In the longitudinally polarized case one should replace in Eq.(3.1) $\gamma^+ \rightarrow \gamma^+ \gamma_5$, and the polarized antiquark distribution is given by the function at $x \rightarrow -x$ without minus sign. In Eq.(3.1) we have dropped the gauge field degrees of freedom (the path-ordered exponential of the gauge field), a step which is justified when working in leading order in the ratio of M

to the UV cutoff, *viz.* the packing fraction of the instanton medium; see Refs.[16, 17] for a detailed discussion.

Thanks to its relativistically invariant definition the matrix element Eq.(3.1) can be evaluated in any frame; for us it is convenient to compute it in the nucleon rest frame. The calculation follows the usual procedure for computing matrix elements of quark bilinears in the chiral quark–soliton model within the $1/N_c$ expansion. The limit $N_c \rightarrow \infty$ justifies the use of the saddle point approximation for the pion field. The matrix element can be calculated with the help of the quark Feynman Green function in the background pion field,

$$G_F(y^0, \mathbf{y}; x^0, \mathbf{x}) = \langle y^0, \mathbf{y} | [i\partial_t - H(U)]^{-1} | x^0, \mathbf{x} \rangle. \quad (3.3)$$

Here the saddle-point pion field is the slowly rotating hedgehog field, Eq.(2.10). For this ansatz the Green function, Eq.(3.3), takes the form

$$[i\partial_t - H(U)]^{-1} = R(t) [i\partial_t - H(U_c) - \Omega]^{-1} R^\dagger(t), \quad (3.4)$$

where Ω is the angular velocity, Eq.(2.11). The matrix element of a quark bilinear between nucleon states of given spin and flavor quantum numbers is obtained by integrating over soliton rotations with wave functions of the collective coordinates, R , corresponding to a given spin/isospin state. In addition, one has to perform a shift of the center of the soliton and integrate over it with plane-wave wave functions in order to obtain a nucleon state of definite three-momentum. This leads to the following expression for the forward matrix element of a color-singlet quark bilinear in the nucleon state (T denotes the time-ordered product):

$$\begin{aligned} & \langle \mathbf{P} = 0, S = T, S_3, T_3 | T \left\{ \psi^\dagger(x) \Gamma \psi(y) \right\} | \mathbf{P} = 0, S = T, S_3, T_3 \rangle \\ &= -2iM_N N_c \int dR_1 \int dR_2 \left[\phi_{T_3 S_3}^{T=S}(R_2) \right]^* \phi_{T_3 S_3}^{T=S}(R_1) \int_{R(-T)=R_1}^{R(T)=R_2} DR \text{Det} [i\partial_t - H(U_c) - \Omega] \\ & \times \int d^3\mathbf{X} \text{Tr} \left[R^\dagger(x^0) \Gamma R(y^0) \langle y^0, \mathbf{y} - \mathbf{X} | [i\partial_t - H(U_c) - \Omega]^{-1} | x^0, \mathbf{x} - \mathbf{X} \rangle \right]. \end{aligned} \quad (3.5)$$

Here Γ denotes a matrix in Dirac spinor and isospin space, and $\text{Tr} \dots$ implies the trace over Dirac and flavor indices (the sum over color indices has already been performed). The path integral over $R(t)$ can be computed using the fact that in the large N_c limit the angular velocity of the soliton, $\Omega = -iR^\dagger \dot{R}$, Eq.(2.11), is suppressed, which allows to expand both the Dirac determinant and the propagator in the integrand in local powers of derivatives of $R(t)$. In particular this expansion gives rise to the kinetic term

$$\exp \left[\frac{i}{2I} \int dt \Omega_a^2(t) \right], \quad (3.6)$$

where I is the moment of inertia of the soliton, Eq.(2.14). The path integral over $R(t)$ with this action can now be computed exactly; it corresponds to the rigid rotator described by the Hamiltonian Eq.(2.12).

When expanding the integrand of the path integral in Eq.(3.5) in powers of Ω we keep all linear terms in Ω in addition to the exponentiated kinetic term. The calculation of the path integral over $R(t)$ is then equivalent to replacing the angular velocity by the spin operator, S , according to the “quantization rule”, Eq.(2.13). When dealing with the matrix element of a non-local bilinear operator as in Eq.(3.5), terms linear in Ω in the integrand of the path integral arise from two sources:

- Expansion of the quark propagator (*cf.* Eq.(3.4)):

$$\begin{aligned} [i\partial_t - H(U_c) - \Omega] \\ = [i\partial_t - H(U_c)]^{-1} + [i\partial_t - H(U_c)]^{-1} \Omega [i\partial_t - H(U_c)]^{-1} + \dots \end{aligned} \quad (3.7)$$

- Expansion of the nonlocal object $R^\dagger(x^0)\Gamma R(y^0)$. This expansion can be performed in two alternative ways:

$$R^\dagger(x^0)\Gamma R(y^0) = R^\dagger(x^0)\Gamma R(x^0) + (y^0 - x^0)R^\dagger(x^0)\Gamma \dot{R}(x^0) + \dots \quad (3.8)$$

$$\text{or} \quad R^\dagger(x^0)\Gamma R(y^0) = R^\dagger(y^0)\Gamma R(y^0) - (y^0 - x^0)\dot{R}^\dagger(y^0)\Gamma R(y^0) + \dots \quad (3.9)$$

It can be shown [9] that both choices lead to the same result for the rotational correction to the matrix element.

Turning now to the calculation of parton distribution functions, defined as matrix elements of the non-local operator Eq.(3.1), it was shown in Ref.[9] that the isosinglet unpolarized distribution, $u(x) + d(x)$, is non-zero already in the leading order of the $1/N_c$ -expansion, *i.e.*, at order Ω^0 in the expansion of the integrand of Eq.(3.5). The isovector unpolarized distribution, on the other hand, appears only in the next-to-leading order, after expanding the integrand to order Ω^1 . It consists of two pieces, which arise, respectively, from the expansion of the propagator, Eq.(3.7), and due to the non-locality of the operator, *cf.* Eq.(3.8),

$$u(x) - d(x) = [u(x) - d(x)]^{(1)} + [u(x) - d(x)]^{(2)}. \quad (3.10)$$

The first contribution from the expansion of the propagator, Eq.(3.7), is given by

$$\begin{aligned} [u(x) - d(x)]^{(1)} &= -\frac{iM_N N_c}{4\pi} \\ &\times \sum_{S_3} \int_{-\infty}^{\infty} dz^0 e^{ixM_N z^0} \int d^3\mathbf{X} \int dR \left[\phi_{T_3 S_3}^{T=S}(R) \right]^* \text{Tr} \left[R^\dagger \tau^3 R (1 + \gamma^0 \gamma^3) \right. \\ &\times \left. \langle z^0, \mathbf{z} - \mathbf{X} | \frac{1}{i\partial_t - H(U_c)} \left(\frac{1}{2I} S^a \tau^a \right) \frac{1}{i\partial_t - H(U_c)} | 0, -\mathbf{X} \rangle \right] \Big|_{z^3=-z^0, z_\perp=0} \phi_{T_3 S_3}^{T=S}(R). \end{aligned} \quad (3.11)$$

The second contribution, originating from the non-locality of the operator, Eq.(3.8), is given by

$$[u(x) - d(x)]^{(2)} = -\frac{iM_N N_c}{4\pi}$$

$$\begin{aligned}
& \times \sum_{S_3} \int_{-\infty}^{\infty} dz^0 e^{ixM_N z^0} \int d^3\mathbf{X} \int dR \left[\phi_{T_3 S_3}^{T=S}(R) \right]^* \text{Tr} \left[z^0 R^\dagger \tau^3 R \frac{i}{2I} S^a \tau^a (1 + \gamma^0 \gamma^3) \right. \\
& \left. \times \langle z^0, \mathbf{z} - \mathbf{X} | \frac{1}{i\partial_t - H(U_c)} | 0, -\mathbf{X} \rangle \right] \Big|_{z^3 = -z^0, z_\perp = 0} \phi_{T_3 S_3}^{T=S}(R). \tag{3.12}
\end{aligned}$$

Here S^a is the spin operator, acting on the rotational wave functions, which enters through the “quantization rule”, Eq.(2.13). Now it is a matter of routine calculations, typical for the chiral quark–soliton model, to compute the rotational matrix elements in Eqs.(3.11, 3.12) and evaluate the functional traces using the basis of eigenfunctions of the Dirac Hamiltonian, Eq.(2.5). The details can be found in Appendix A. The result for the first contribution, Eq.(3.11), is

$$\begin{aligned}
[u(x) - d(x)]^{(1)} &= (2T^3) \frac{N_c M_N}{12I} \\
&\times \left\{ 2 \sum_{\text{occup.}} \sum_{E_m \neq E_n} \frac{1}{E_m - E_n} \langle n | \tau^a | m \rangle \langle m | \tau^a (1 + \gamma^0 \gamma^3) \delta(E_n + P^3 - xM_N) | n \rangle \right. \\
&\left. - \sum_{\text{occup.}} \sum_{E_m = E_n} \langle n | \tau^a | m \rangle \langle m | \tau^a (1 + \gamma^0 \gamma^3) \delta'(E_n + P^3 - xM_N) | n \rangle \right\}, \tag{3.13}
\end{aligned}$$

where $T^3 = \pm 1/2$ is the isospin projection of the nucleon. Eq.(3.13) expresses the isovector distribution as a sum over quark single–particle levels in the background pion field, *cf.* Eq.(2.4). In the first term on the R.H.S. of Eq.(3.13) the outer sum over n runs over all occupied levels, including the bound–state level as well as the negative Dirac continuum, while the inner sum runs over *all* levels with the restriction that $E_m \neq E_n$.² This formula assumes a quasi–discrete spectrum and can be directly applied to numerical calculations in a finite box; for the continuum case see Appendix A. The second contribution, Eq.(3.12), can be expressed through the derivative of the *isosinglet* quark distribution, calculated in leading order of the $1/N_c$ –expansion:

$$\begin{aligned}
[u(x) - d(x)]^{(2)} &= -(2T^3) \frac{N_c}{4I} \times \frac{\partial}{\partial x} \sum_{\text{occup.}} \langle n | (1 + \gamma^0 \gamma^3) \delta(E_n + P^3 - xM_N) | n \rangle \\
&= -(2T^3) \frac{1}{4IM_N} \times \frac{\partial}{\partial x} [u(x) + d(x)]^{\text{leading}}. \tag{3.14}
\end{aligned}$$

We note that, as in the case of the isosinglet distribution [9, 10], there exists an equivalent representation of the isovector distribution as a sum over *non-occupied* levels (see Appendix A):

$$[u(x) - d(x)]^{(1)} = -(2T^3) \frac{N_c M_N}{12I}$$

²Here, as in Eqs.(2.6, 2.14), the sums over n, m denote the sum over all quantum numbers characterizing the single–particle states; note that the energy eigenvalues are in general degenerate in the third component of the “grand spin”, the sum of the quark angular momentum and isospin [6].

$$\times \left\{ 2 \sum_{\substack{n \\ \text{non-occup.}}} \sum_{\substack{m \\ E_m \neq E_n}} \frac{1}{E_m - E_n} \langle n | \tau^a | m \rangle \langle m | \tau^a (1 + \gamma^0 \gamma^3) \delta(E_n + P^3 - x M_N) | n \rangle \right. \\ \left. - \sum_{\substack{n \\ \text{non-occup.}}} \sum_{\substack{m \\ E_m = E_n}} \langle n | \tau^a | m \rangle \langle m | \tau^a (1 + \gamma^0 \gamma^3) \delta'(E_n + P^3 - x M_N) | n \rangle \right\}, \quad (3.15)$$

$$[u(x) - d(x)]^{(2)} = (2T^3) \frac{N_c}{4I} \times \frac{\partial}{\partial x} \sum_{\substack{n \\ \text{non-occup.}}} \langle n | (1 + \gamma^0 \gamma^3) \delta(E_n + P^3 - x M_N) | n \rangle. \quad (3.16)$$

In both Eqs.(3.13, 3.14) and (3.15, 3.16) vacuum subtraction, *i.e.*, subtraction of the corresponding sums over vacuum levels ($U = 1$) and with vacuum occupation numbers, is understood. It can be shown that vacuum subtraction is required only for $x < 0$ in the sum over occupied, and for $x > 0$ in the sum over non-occupied levels. This fact is important for the numerical calculations: we shall use the representation as a sum over occupied states for $x > 0$, and as a sum over non-occupied states for $x < 0$ (see below).

The two contributions to the isovector distribution function, Eq.(3.13) and Eq.(3.14), which have emerged from the expansion of the integrand of Eq.(3.5), both contain delta function type singularities at $x = 0$. For the second contribution, Eq.(3.14), this is immediately obvious: the isosinglet distribution is discontinuous at $x = 0$, so its derivative contains a delta function centered at $x = 0$. In a similar way one can convince oneself that also the second term in Eq.(3.13) exhibits such a singularity. These delta function singularities cancel when the two contributions are added, *cf.* Eq.(3.10). For the numerical calculations it is convenient to regroup the terms in such a way that this cancellation happens at the level of analytical expressions, *i.e.*, that the singular terms are combined in one term. By inserting intermediate states this term can be expressed as a double sum over levels, similar to the first term on the L.H.S. of Eq.(3.13). Doing this simple rearrangement one obtains

$$[u(x) - d(x)] = [u(x) - d(x)]^{(1')} + [u(x) - d(x)]^{(2')}, \quad (3.17)$$

$$[u(x) - d(x)]^{(1')} = (2T^3) \frac{N_c M_N}{6I} \\ \times \sum_{\substack{n \\ \text{occup.}}} \sum_{\substack{m \\ E_m \neq E_n}} \frac{1}{E_m - E_n} \langle n | \tau^a | m \rangle \langle m | \tau^a (1 + \gamma^0 \gamma^3) \delta(E_n + P^3 - x M_N) | n \rangle, \quad (3.18)$$

$$[u(x) - d(x)]^{(2')} = -(2T^3) \frac{N_c}{12I} \\ \times \frac{\partial}{\partial x} \sum_{\substack{n \\ \text{occup.}}} \sum_{\substack{m \\ E_m \neq E_n}} \langle n | \tau^a | m \rangle \langle m | \tau^a (1 + \gamma^0 \gamma^3) \delta(E_n + P^3 - x M_N) | n \rangle, \quad (3.19)$$

and a corresponding representation as sums over non-occupied states, *cf.* Eqs.(3.15, 3.16). The expressions for the distribution function Eqs.(3.17, 3.18 3.19) will be used in the actual numerical calculations.

We would like to comment on a recent calculation of the isovector distribution in the chiral quark–soliton model by Wakamatsu and Kubota [19], who follow basically the same approach as we do here. However, in the expansion of the integrand of the path integral over soliton rotations, Eq.(3.5), these authors drop the terms arising due to the non-locality of the quark bilinear operator, Eq.(3.19). They argue that the non-locality of this operator is of the order of the inverse large momentum transfer in deep–inelastic scattering, $1/Q$, so that the slow rotational motion of the soliton does not affect the operator. This argument, however, seems not appropriate: the light–like separation between the quark fields in the operator for the parton distribution is governed by the Bjorken variable x (more precisely, by xM_N), not by the momentum transfer Q^2 . After factorization of the DIS cross section in QCD the hard momentum enters only in the coefficient functions, which can be computed perturbatively, not in the operator for the parton distribution functions. Hence there is no reason to drop the contribution Eq.(3.19) from the Ω –expansion, the more that the non-locality of the quark bilinear operator is taken into account at other places in the calculation of the parton distribution.

The authors of Ref.[19] also argue that in the contribution Eq.(3.18) the double sum over levels should be restricted to include only transitions from occupied to non-occupied states, since transitions from occupied to occupied states, as are present in Eq.(3.18) (*cf.* the derivation in Appendix A) would violate the Pauli principle. While this argument is correct for local operators, we are dealing here with an operator non-local in time, for which this so-called Pauli blocking is not restrictive. We thus see no reason for dropping the occupied–to–occupied transitions in the double sum over levels in Eq.(3.18). Indeed, it turns out that the full expression Eq.(3.18) is required to ensure equivalence of summation over occupied and non-occupied states, as will be discussed below.

The dropping of the contribution Eq.(3.19) to the parton distribution function in Ref.[19] has rather drastic consequences. One may expect the differences to the full result to be most significant at small values of x , since they correspond to large light–like separations of the bilinear operator. To illustrate the differences we have performed a numerical calculation of the distribution function following the prescription of Ref.[19] and compared the results to those of our calculation, where we take into account all terms. [The details of the numerical calculations and the ultraviolet regularization are given below in Subsection 3.2 and Section 4.] Fig.1 shows the contribution of the negative Dirac continuum to the sum over n in in Eqs.(3.18, 3.19) in both cases. One sees that the two distributions differ strongly. The full result (solid line), corresponding to the sum of Eqs.(3.18) and (3.19), is large at $x = 0$ and vanishes rapidly for larger values of x . The result obtained after dropping Eq.(3.19), as done in Ref.[19], is shown by the dashed line; in this case the distribution is small at $x = 0$ and does not vanish for large values of x .

To conclude this discussion, we note that the truncations made in Ref.[19] seem problematic in yet another respect. The calculation of the parton distribution in Ref.[19] starts from the bilinear operator $\bar{\psi} \dots \psi$; however, one may just as well take the opposite ordering of the operator, $-\psi \dots \bar{\psi}$. In QCD the two orderings give equivalent expressions for the parton distribution, thanks to the anticommutativity of the fermion fields at space–like separations. In the chiral quark–soliton model, the two orderings lead, respectively, to representations

of the parton distribution as sums over occupied and non-occupied quark single-particle states. The equivalence between these two representations holds only for the full expression for the distribution as it derives from Eq.(3.5), *i.e.*, for the sum of *all* terms in the expansion with respect to angular velocity; see Appendix A. Consequently, dropping the contribution Eq.(3.19) (or otherwise truncating the sums over levels) one violates this equivalence. We have verified this in the numerical calculations. For the full result (the solid line in Fig.1) we observe equivalence of summation over positive and negative energy states, but not for the distribution computed according to the prescription of Ref.[19] (the dashed line in Fig.1) when computed by summing instead over positive-energy states.

3.2 Ultraviolet regularization

In the previous section we have obtained expressions for the isovector quark distribution as sums over quark single particle levels in the background pion field. In Eqs.(3.18, 3.19) the sum over n runs over all occupied levels, that is, the discrete bound-state level and the negative Dirac continuum, schematically

$$\sum_{\substack{n \\ \text{occup.}}} [\dots] = [\dots]_{n=\text{lev}} + \sum_{\substack{n \\ \text{neg.cont.}}} [\dots], \quad (3.20)$$

where the ellipsis denotes the “inner” sum over m with the restriction that $E_m \neq E_n$. We shall refer to the two terms on the R.H.S. of Eq.(3.20) as the “level” and “continuum” contributions. One should keep in mind, however, that this distinction is quite formal, and that only the total sum over occupied (or, equivalently, non-occupied) states has physical significance.

In the derivation of the expressions for the quark distribution function we have so far not taken into account the ultraviolet cutoff intrinsic in the effective chiral theory. In fact, the expressions for the isovector distribution, Eqs.(3.13, 3.14) *viz.* Eqs.(3.18, 3.19), contain an ultraviolet divergence due to the Dirac continuum contribution, and thus require regularization. Quite generally, in a calculation of parton distribution functions there are very strong restrictions on how one should introduce the UV cutoff in the effective theory. The point is that one has to preserve certain general properties of parton distributions such as positivity, sum rules *etc.*, which can easily be violated by an arbitrary UV regularization. Specifically, the regularization should preserve the completeness of the set of quark single-particle wave functions in the soliton pion field. One possible regularization method which fulfills all requirements is a Pauli–Villars subtraction, which was used in the calculations of the N_c -leading distributions in Refs.[9, 10, 11]. We shall also employ this method here. Thus, we regularize Eqs.(3.13, 3.14) *viz.* Eqs.(3.18, 3.19) as follows:

$$[u(x) - d(x)]_{\text{reg.}} = [\dots]_{n=\text{lev}, M} + \left(\sum_{\substack{n \\ \text{neg.cont.}}} [\dots]_M - \frac{M^2}{M_{PV}^2} \sum_{\substack{n \\ \text{neg.cont.}}} [\dots]_{M_{PV}} \right), \quad (3.21)$$

where the subscript M_{PV} denotes the corresponding expression computed with the constituent quark mass, M , replaced by the regulator mass, M_{PV} , *cf.* Eqs.(2.8, 2.9). This

subtraction removes the logarithmic divergence of the distribution function, as can be shown using methods similar to those developed in Ref.[10] (gradient expansion). We do not include the contribution of the discrete level to the isovector distribution in the Pauli–Villars subtraction; this contribution is finite and does not need to be subtracted.

The moment of inertia of the soliton, Eq.(2.14), is also ultraviolet divergent. It must be regularized consistently with the isovector distribution in order to preserve the isospin sum rule (see Subsection 3.3). This is achieved by regularizing it by a Pauli–Villars subtraction analogous to Eq.(3.21).

We stress again that the calculation of parton distributions in the effective chiral theory, *i.e.*, the identification of the twist–2 QCD operator with an operator expressed in terms of fields of the effective theory, Eq.(3.1), is based on the parametric smallness of the ratio of the constituent quark mass, M , to the ultraviolet cutoff (here: M_{PV}). The approach is consistent in the sense that the expressions for the parton distributions in the effective theory are logarithmically divergent and thus insensitive to the details of the ultraviolet regularization (assuming that the latter does not violate any important properties such as completeness *etc.*). It should be noted, however, that the lack of precise knowledge of the “true” ultraviolet regularization leads to a theoretical uncertainty at the level of finite terms, $\propto M^2/M_{PV}^2$. For instance, Pauli–Villars subtraction of the finite level contribution would correspond to a modification of the distribution function by an amount of order M^2/M_{PV}^2 . The numerical results presented in Section 4 should be understood as a calculation of the parton distributions with a typical regularization fulfilling all general requirements, with the theoretical uncertainty in the ultraviolet regularization leading to a numerical uncertainty of typically 10–20 % — except for the sum rules, which follow from general principles not violated by the ultraviolet regularization.

3.3 The isospin sum rule

We now want to demonstrate that the expressions derived for the isovector distribution in the chiral quark–soliton model are consistent with the isospin sum rule,

$$\int_{-1}^1 dx [u(x) - d(x)] \equiv \int_0^1 dx [u(x) - \bar{u}(x) - d(x) + \bar{d}(x)] = 2T_3. \quad (3.22)$$

Consider the representation of the isovector distribution function as a sum over quark levels, Eqs.(3.18, 3.19). Since the contribution $[u(x) - d(x)]^{(2')}$, Eq.(3.19), is a total derivative, it does not contribute to the integral in Eq.(3.22), and we can concentrate on the contribution $[u(x) - d(x)]^{(1')}$, Eq.(3.18). Integrating Eq.(3.18) over x , replacing in the large- N_c limit the integral from -1 to 1 by the integral over the whole real axis, we use up the delta functions in Eq.(3.19) and obtain

$$\int_{-1}^1 dx [u(x) - d(x)] = (2T_3) \frac{N_c}{6I} \sum_{\text{occup.}} \sum_{\substack{m \\ E_m \neq E_n}} \frac{\langle n | \tau^a | m \rangle \langle m | \tau^a | n \rangle}{E_m - E_n}. \quad (3.23)$$

The hedgehog symmetry of the pion field, Eq.(2.3), has allowed us to drop the $\gamma^0\gamma^3$ -term. Taking into account that the soliton moment of inertia, Eq.(2.14), can equivalently be written as

$$I = \frac{N_c}{6} \sum_{\substack{n \\ \text{occup.}}} \sum_{\substack{m \\ E_m \neq E_n}} \frac{\langle n | \tau^a | m \rangle \langle m | \tau^a | n \rangle}{E_m - E_n}, \quad (3.24)$$

we immediately reproduce the isospin sum rule, Eq.(3.22). Also, it can be seen that the Pauli–Villars regularization of the distribution function and the moment of inertia as defined by Eq.(3.21) does not upset this proof; in particular, it preserves the equivalence of the two representations of the moment of inertia, Eq.(2.14) and Eq.(3.24).

3.4 The Gottfried sum

An interesting quantity related to the isovector antiquark distribution is the Gottfried sum [14, 15], which is defined as

$$I_G = \frac{1}{3} + \frac{2}{3} \int_0^1 dx [\bar{u}(x) - \bar{d}(x)]. \quad (3.25)$$

The integral on the R.H.S. is scale-dependent only at two-loop level; its scale dependence is negligible over the entire perturbative region. If the sea quark distribution were isospin symmetric, $\bar{u}(x) = \bar{d}(x)$, which would be the case if, for example, one assumed the sea quark distribution to be generated entirely radiatively, this quantity would be equal to 1/3 (Gottfried sum rule). However, the NMC experiment [24] finds a significant deviation from this value,

$$I_G = 0.235 \pm 0.026 \quad \text{at} \quad Q^2 = 4 \text{ GeV}^2, \quad (3.26)$$

indicating that the sea quark distribution is rather far from flavor-symmetric. Note that the Gottfried sum rule does not follow from any fundamental principles of QCD. In fact, the large- N_c picture of the nucleon as a chiral soliton naturally explains the presence of a flavor-nonsymmetric antiquark distribution.

The expression for the Gottfried sum in the chiral quark-soliton model is obtained by integrating the expression for the total isovector quark distribution, Eqs.(3.18, 3.19), over x from -1 to 0 , keeping in mind that the antiquark distribution is given by minus the expressions in Eqs.(3.18, 3.19) at $-x$. Since the integration extends only over half of the x -axis, also the total derivative term, Eq.(3.19), contributes to the Gottfried sum, in contrast to the isospin sum rule, Eq.(3.22), where the integration runs over the whole x -axis and Eq.(3.14) drops out. This contribution to the Gottfried sum in the chiral quark-soliton model has not been mentioned in Ref.[9].

We refrain from writing down the analytic expressions for the Gottfried sum obtained by integrating Eqs.(3.13, 3.14). Instead, we shall compute Eq.(3.25) by integration of the numerically computed antiquark distribution function, see below. In particular, the ultraviolet regularization of the Gottfried sum and all other properties will follow directly from that of the distribution functions.

We note that the Gottfried sum in the large- N_c limit has been discussed previously in the context of the chiral quark-soliton model [25] and the Skyrme model [26]. These studies were, however, based on expressions for the R.H.S. of Eq.(3.25) which do not follow from a consistent identification of the isovector distribution function within the effective model.

4 Numerical results and discussion

The method we choose for the numerical computation of the isovector unpolarized distribution function parallels that for computing the isosinglet unpolarized one [10]. We evaluate the sums over quark single-particle levels in the background pion field by placing the soliton in a spherical 3-dimensional box, where the eigenfunctions of the Dirac Hamiltonian in the background pion field can be obtained by numerical diagonalization [27]. To facilitate the calculations we first convert the expressions Eqs.(3.18, 3.19) to a spherically symmetric form by averaging over the 3-dimensional orientations of the spatial separation implied in the non-local operator Eq.(3.1), see Ref.[10] for details. In the spherically symmetric version of Eqs.(3.18, 3.19) the matrix elements of the operators between single-particle quark states can easily be computed using the standard angular-momentum selection rules. The discontinuous functions of the single-particle energies and the single-particle momentum operator, which arise as a consequence of the presence in Eqs.(3.18, 3.19) of the functions $\delta(E_n + P^3 - xM_N)$, are smoothed using the “smearing” method of Ref.[10].³

For the ultraviolet regularization of distribution functions we employ the Pauli-Villars subtraction, Eq.(3.21). For the sake of numerical stability we first evaluate the sums over levels Eqs.(3.18, 3.19) with a smooth energy cutoff, both the sums over levels obtained with the usual quark mass, M , and the regulator mass, M_{PV} . We then perform the Pauli-Villars subtraction, Eq.(3.21), and remove the energy cutoff by extrapolation to infinity.

We have calculated the isovector quark distribution for two values of the constituent quark mass, $M = 350$ MeV, which is the value obtained in Ref.[5] for the instanton vacuum, and $M = 420$ MeV. The ultraviolet cutoff is in both cases determined by fitting the pion decay constant, Eq.(2.9), $M_{PV}^2/M^2 = 2.52$ ($M = 350$ MeV) and $M_{PV}^2/M^2 = 1.90$ ($M = 420$ MeV). The soliton profile, Eq.(2.3), and the nucleon mass have been found by self-consistent minimization of the Pauli-Villars regularized static energy in Ref.[11], $M_N = 1140$ MeV ($M = 350$ MeV) and $M_N = 1040$ MeV ($M = 420$ MeV). A number of other hadronic nucleon observables such as the isovector axial coupling constant $g_A^{(3)}$ have been calculated with this ultraviolet regularization in Ref.[21]. The results for the isovector unpolarized quark and antiquark distributions are shown in Figs.2–4.

Before comparing our results with the parametrizations of the experimental data it is instructive to study the behavior of the different contributions to the distribution function in

³The contribution Eq.(3.18) to the isovector distribution function is a double sum over quark single-particle levels, similar to the moment of inertia, Eq.(2.14). In the evaluation of these quantities in a finite box there arises the complication that the boundary conditions which have to be imposed on the single-particle wave functions can lead to spurious “vacuum” contributions. In Ref.[28] a method has been devised to circumvent this problem by using two sets of basis functions in the box subject to different boundary conditions. We have employed this technique in the calculations of distribution functions reported here.

this model. Fig.2 shows the function $u(x) - d(x)$ for both positive and negative x , describing the isovector quark distribution at positive and minus the antiquark distribution at negative values of x . The dashed line shows the contribution of the discrete level, as defined by Eq.(3.20). This contribution is concentrated around values $x \sim 1/3$ and similar in shape to the bound-state level contribution to the isosinglet unpolarized and isovector polarized distributions [10, 11]. The contribution of the Dirac continuum, *cf.* Eq.(3.20), is shown by the dot-dashed line. Similar to the isosinglet distribution this contribution is peaked around $x = 0$; however, in the isovector case this function does not change sign at $x = 0$. The total is given by the solid line; one observes that it is essentially a smooth function except for a region of x around $x = 0$, where it is dominated by the Dirac continuum contribution. Note also that the calculated distribution satisfies the isospin sum rule, as discussed in Subsection 3.3 (the area under the solid line in Fig.2 is unity).

The isovector quark and antiquark distributions calculated here refer to a low normalization point of the order of the cutoff of the effective chiral theory ($\simeq 600$ MeV), and can be compared to experimental data for structure functions only after perturbative evolution to larger scales. Hence the “small- x ” behavior of the calculated parton distribution apparent from Fig.2 has significance only in the sense of an input distribution at a low scale and does not imply a statement about the small- x behavior of the structure functions at experimental scales.

The parton distribution functions calculated in the effective theory are but logarithmically divergent with the UV cutoff and thus, for typical values of x , insensitive to the details of the UV cutoff (assuming a physically acceptable regularization scheme meeting the criteria discussed above). However, it is known that in the parametrically small region $|x| \leq (M/\Lambda)^2/N_c$ the shape of the distribution depends on the details of the UV regularization, as has recently been discussed in connection with the calculation of off-forward parton distributions in this approach [13]. For instance, it was seen there that the discontinuity at $x = 0$ of the isosinglet distribution calculated with Pauli-Villars regularization is reduced to a smooth transition when the regularization is implemented in the form of a momentum-dependent constituent quark mass, as suggested by the instanton vacuum. [For values of x not in the vicinity of zero results are practically unchanged as compared to the Pauli-Villars regularization.] One may thus surmise that also the shape of the peak in the isovector distribution at $x = 0$ depends strongly on the ultraviolet cutoff. The calculation of the $1/N_c$ -suppressed distribution functions with regularization by a momentum-dependent mass is outside the scope of the presently available methods. The interesting general problem of the relation of the ultraviolet cutoff of the effective theory to the “small- x ” behavior of the low-scale parton distributions will be left for further investigation.

In Fig.3 we compare the distribution functions obtained for two different values of the constituent quark mass, $M = 350$ MeV and $M = 420$ MeV. With the ultraviolet regularization chosen according to Eqs.(2.8, 2.9) and Eq.(3.21), and the soliton profile determined by minimization of the energy Eq.(2.8), the only remaining free parameter in this model calculation is the value of the constituent quark mass, M . Rather than trying to determine an “optimum” value by performing a best fit to a number of hadronic observables, it is more interesting here to study the dependence of the calculated parton distributions on this

M	$\int_0^1 dx [\bar{u}(x) - \bar{d}(x)]$			I_G
	level	continuum	total	
350 MeV	0.030	-0.201	-0.171	0.219
420 MeV	0.049	-0.281	-0.232	0.178

Table 1: The integral of the antiquark distribution and the Gottfried sum, Eq.(3.25), for constituent quark masses 350 MeV and 420 MeV. *Columns 2–4*: integral of the antiquark distribution, $\int_0^1 dx [\bar{u}(x) - \bar{d}(x)]$: contribution of the discrete level, the Dirac continuum and the total result, *cf.* Fig.2. *Column 5*: Gottfried sum, Eq.(3.25). The experimental value quoted in Ref.[24] is $I_G = 0.235 \pm 0.026$ at $Q^2 = 4 \text{ GeV}^2$.

parameter. Fig.3 gives an idea of the variation of the results with M .

The parton distributions computed here should be used as input for perturbative evolution, starting with a scale of the order of the cutoff ($\simeq 600 \text{ MeV}$). We shall not perform the evolution here, but rather compare our results with the parameterizations by Glück, Reya, and Vogt [18]. These authors generate parton distributions at experimental Q^2 from “valence-like” (non-singular) input quark-, antiquark and gluon distributions at a normalization point of the order of 600 MeV and obtain excellent fits to the data from deep-inelastic scattering and a variety of other processes. In Fig.4 we compare the isovector distribution of quarks, $x[u(x) - d(x)]$, and antiquarks, $x[\bar{u}(x) - \bar{d}(x)]$, to the GRV parametrization [18]. One notes that the calculated distributions are systematically harder (*i.e.*, centered at larger values of x) than the GRV one, indicating that the normalization point of the calculated distributions is even lower than that of the GRV parametrization. This is consistent with the conclusions drawn from the comparison of the isosinglet unpolarized [9, 10, 11] and isovector polarized [9, 10] distributions to the GRV parametrizations; however, in the isovector unpolarized case considered here the comparison of the calculated distribution with the GRV fit is more direct since, contrary to the isosinglet unpolarized distribution, this distribution does not mix with the gluon distribution under evolution, and its normalization is scale-independent. [Also, contrary to the isovector polarized distribution whose normalization is given by the isovector axial coupling constant, $g_A^{(3)}$, whose value in our approach is model-dependent, the normalization of the the isovector unpolarized distribution is universal thanks to the isospin sum rule.]

Note that the order of magnitude and shape of the calculated isovector antiquark distribution are in good agreement with the GRV parametrization, see Fig.4. As can be seen from Fig.2 the antiquark distribution is dominated by the Dirac continuum contribution. We note that our distribution differs significantly from the result of Ref.[19], where the contribution from the term Eq.(3.19) has been dropped; our distribution vanishes rapidly for large x , in contrast to the one of Ref.[19], see Fig.1.

With regard to the isovector antiquark distribution it is interesting to compute the Gottfried sum, Eq.(3.25). The results for the two constituent quark masses $M = 350 \text{ MeV}$ and $M = 420 \text{ MeV}$ are given in Table 1, where we also list separately the contributions of the

discrete level and the Dirac continuum to the integral from of the antiquark distribution. As can be seen, the deviation of the Gottfried sum from $1/3$ is dominated by the Dirac continuum contribution. The values are in reasonable agreement with the NMC value [24]. We note that, since our Dirac continuum contribution strongly differs from that of Ref.[19], the good agreement of the value of I_G reported there with experiment seems fortuitous.

Finally, we note that the parton distributions studied here refer to the large- N_c limit, where the nucleon is heavy, $M_N \propto N_c$. The calculated distributions therefore do not go to zero at $x = 1$, rather, they are exponentially small at large x , as discussed in Ref.[9]. For this reason we have evaluated the integral of the antiquark distribution in Eq.(3.25) and Table 1 with the upper limit replaced by infinity. Numerically, the contribution from values of $x > 1$ to the integral is negligible.

5 Conclusions

In this paper we have extended the approach to calculate parton distributions at a low normalization point in the large- N_c limit to the case of the distributions which appear in the subleading order of the $1/N_c$ -expansion. Specifically, we have computed the isovector unpolarized distribution of quarks and antiquarks. The methods developed here can readily be generalized to compute also the other $1/N_c$ -subleading distributions, namely the isosinglet longitudinally and transverse polarized ones, as well as the rotational $1/N_c$ -corrections to the isovector polarized distribution. These distributions are currently being computed.

We have found reasonable agreement of the calculated distributions with the parametrizations of the data at a low normalization point. In particular, the large- N_c approach naturally predicts a flavor-asymmetric (*i.e.*, non-radiative) sea quark distribution of correct sign and magnitude. The x -dependence of the isovector antiquark distribution compares well with the GRV parametrizations. It is interesting that the calculated distributions exhibit a strong rise at $x = 0$. Also, the integral of the calculated isovector antiquark distribution (the violation of the Gottfried sum rule) is compatible with the experimental data, in view of the general theoretical uncertainties of the present approach.

Acknowledgements

The authors are deeply grateful to D.I. Diakonov and V.Yu. Petrov for many enlightning conversations.

This work has been supported in part by a joint grant of the Russian Foundation for Basic Research (RFBR) and the Deutsche Forschungsgemeinschaft (DFG) 436 RUS 113/181/0 (R), by RFBR grant 96-15-96764, by the NATO Scientific Exchange grant OIUR.LG 951035, by INTAS grants 93-0283 EXT and 93-1630-EXT, by the DFG and by COSY (Jülich). The Russian participants acknowledge the hospitality of Bochum University.

A Evaluation of the isovector distribution

In this appendix we evaluate the two contributions to the isovector distribution arising from the expansion in angular frequency, Eqs.(3.11) and (3.12). Our aim is to express these contributions in the form of sums over quark single-particle levels, which *e.g.* can serve as a starting point for a numerical calculation of the distribution function.

We begin by rewriting the contributions Eqs.(3.11) and (3.12) in the form

$$\begin{aligned}
[u(x) - d(x)]^{(1)} &= \\
& -\frac{N_c M_N i}{8\pi I} \sum_{S_3} \int_{-\infty}^{\infty} dz^0 e^{ix M_N z^0} \int d^3 \mathbf{X} \int dR \left[\phi_{T_3 S_3}^{T=S}(R) \right]^* D_{3b}(R) S^a \phi_{T_3 S_3}^{T=S}(R) \\
& \times \text{Tr} \left[\tau^b (1 + \gamma^0 \gamma^3) \langle z^0, \mathbf{z} - \mathbf{X} | \frac{1}{i\partial_t - H(U_c)} \tau^a \frac{1}{i\partial_t - H(U_c)} | 0, -\mathbf{X} \rangle \right] \Big|_{z^3 = -z^0, z_{\perp} = 0},
\end{aligned} \tag{A.1}$$

$$\begin{aligned}
[u(x) - d(x)]^{(2)} &= \\
& \frac{M_N N_c}{8\pi I} \sum_{S_3} \int_{-\infty}^{\infty} dz^0 e^{ix M_N z^0} \int d^3 \mathbf{X} \int dR \left[\phi_{T_3 S_3}^{T=S}(R) \right]^* z^0 D_{3b}(R) S^c \\
& \times \text{Tr} \left[\tau^b \tau^c (1 + \gamma^0 \gamma^3) \langle z^0, \mathbf{z} - \mathbf{X} | \frac{1}{i\partial_t - H(U_c)} | 0, -\mathbf{X} \rangle \right] \Big|_{z^3 = -z^0, z_{\perp} = 0} \phi_{T_3 S_3}^{T=S}(R),
\end{aligned} \tag{A.2}$$

where $\text{Tr} \dots$ denotes the trace over Dirac and flavor indices. Here we have introduced the Wigner D -function in the vector representation

$$D_{ab}(R) = \frac{1}{2} \text{Tr} (\tau_a R \tau_b R^\dagger). \tag{A.3}$$

We first have to compute the rotational matrix element. Strictly speaking, this matrix element contains noncommuting operators, $D_{3b}(R)$ and S^a , and one should be careful about their ordering. However, due to the average over the nucleon spin the result does not depend on the order, and one has

$$\begin{aligned}
& \sum_{S_3} \int dR \left[\phi_{T_3 S_3}^{T=S}(R) \right]^* D_{3b}(R) S^a \phi_{T_3 S_3}^{T=S}(R) \\
& = \sum_{S_3} \int dR \left[\phi_{T_3 S_3}^{T=S}(R) \right]^* S^a D_{3b}(R) \phi_{T_3 S_3}^{T=S}(R) = -\frac{1}{3} \delta^{ab} (2T^3).
\end{aligned} \tag{A.4}$$

Using this, and passing from the time to the frequency representation for the quark Green functions we arrive at

$$\begin{aligned}
[u(x) - d(x)]^{(1)} &= (2T^3) \frac{i N_c M_N}{24\pi I} \int_{-\infty}^{\infty} dz^0 e^{ix M_N z^0} \int \frac{d\omega}{2\pi} e^{-i\omega z^0} \int d^3 \mathbf{X} \\
& \times \text{Tr} \left[\tau^a (1 + \gamma^0 \gamma^3) \langle \mathbf{z} - \mathbf{X} | \frac{1}{\omega - H(U_c)} \tau^a \frac{1}{\omega - H(U_c)} | -\mathbf{X} \rangle \right] \Big|_{z^3 = -z^0, z_{\perp} = 0},
\end{aligned} \tag{A.5}$$

$$\begin{aligned}
[u(x) - d(x)]^{(2)} &= -(2T^3) \frac{N_c M_N}{8\pi I} \int_{-\infty}^{\infty} dz^0 e^{ixM_N z^0} z^0 \int \frac{d\omega}{2\pi} e^{-i\omega z^0} \int d^3\mathbf{X} \\
&\times \text{Tr} \left[(1 + \gamma^0 \gamma^3) \langle \mathbf{z} - \mathbf{X} | \frac{1}{\omega - H(U_c)} | -\mathbf{X} \rangle \right] \Big|_{z^3 = -z^0, z_{\perp} = 0}.
\end{aligned} \tag{A.6}$$

[The treatment of the poles in the ω -integral implied here will be described below.] These expressions have the form of an integral over all space of a matrix element of the quark propagator between position eigenstates localized at different points. It is convenient to rewrite them as functional traces (*i.e.*, sums over diagonal matrix elements) by introducing the finite translation operator, which is given as the exponential of the single-particle momentum operator, P^k ,

$$\langle \mathbf{z} - \mathbf{X} | = \langle -\mathbf{X} | \exp(iP^k z^k). \tag{A.7}$$

We can then perform the integral over z^0 and write the result in the form

$$\begin{aligned}
[u(x) - d(x)]^{(1)} &= \\
(2T^3) \frac{iN_c M_N}{24\pi I} \int_{-\infty}^{\infty} d\omega \text{Sp} \left[\tau^a (1 + \gamma^0 \gamma^3) \delta(\omega + P^3 - xM_N) \frac{1}{\omega - H(U_c)} \tau^a \frac{1}{\omega - H(U_c)} \right],
\end{aligned} \tag{A.8}$$

$$[u(x) - d(x)]^{(2)} = (2T^3) \frac{iN_c}{8\pi I} \frac{\partial}{\partial x} \int_{-\infty}^{\infty} d\omega \text{Sp} \left[(1 + \gamma^0 \gamma^3) \delta(\omega + P^3 - xM_N) \frac{1}{\omega - H(U_c)} \right], \tag{A.9}$$

where $\text{Sp} \dots$ denotes the functional trace in the space of single-particle quark states. These functional traces can now be computed using a basis of eigenstates of the Dirac Hamiltonian in the background pion field, Eq.(2.4). As to the second contribution, Eq.(A.9), one may easily show that, up to a factor, it is simply the derivative in x of the isosinglet distribution function, which appears in the leading order of the $1/N_c$ -expansion [9, 10]. It can be written as a simple sum over occupied single-particle levels:

$$\begin{aligned}
[u(x) - d(x)]^{(2)} &= -(2T^3) \frac{1}{4IM_N} \times \frac{\partial}{\partial x} [u(x) + d(x)]^{\text{leading}} \\
&= -(2T^3) \frac{N_c}{4I} \times \frac{\partial}{\partial x} \sum_{\text{occup.}} \langle n | (1 + \gamma^0 \gamma^3) \delta(E_n + P^3 - xM_N) | n \rangle.
\end{aligned} \tag{A.10}$$

It is also possible to express this quantity as a sum over non-occupied levels, Eq.(3.16), see Refs.[9, 10].

Let us now consider the first contribution, Eq.(A.8). It gives rise to a double sum over levels,

$$\begin{aligned}
[u(x) - d(x)]^{(1)} &= (2T_3) \frac{iN_c M_N}{24\pi I} \int_{-\infty}^{\infty} d\omega \sum_{m,n} \langle n | \tau^a (1 + \gamma^0 \gamma^3) \delta(\omega + P^3 - xM_N) | m \rangle \\
&\quad \times \langle m | \tau^a | n \rangle \frac{1}{(\omega - E_m)(\omega - E_n)},
\end{aligned} \tag{A.11}$$

where the sums over n, m run over all levels. We can further simplify the form of Eq.(A.11) by taking into account that the expression on the R.H.S. is real. First, this is natural, since the quark distribution function, $u(x) - d(x)$, must be real. More formally, one may prove the reality of the R.H.S. of Eq.(A.11) starting from the locality of the Dirac Hamiltonian in the background field, and the fact that neither the angular velocity corrections to the Hamiltonian nor our ultraviolet regularization violate this property. We may thus replace the expression on the R.H.S. of Eq.(A.11) by its real part:

$$\begin{aligned}
[u(x) - d(x)]^{(1)} &= \\
&= -(2T^3) \frac{N_c M_N}{24\pi I} \text{Im} \int_{-\infty}^{\infty} d\omega \sum_{m,n} \langle n | \tau^a (1 + \gamma^0 \gamma^3) \delta(\omega + P^3 - xM_N) | m \rangle \\
&\quad \times \langle m | \tau^a | n \rangle \frac{1}{[\omega - E_m + i0\eta(E_m)][\omega - E_n + i0\eta(E_n)]}.
\end{aligned} \tag{A.12}$$

Here the poles in the ω -integral corresponding to the single-particle energies are shifted according to the occupation of the levels

$$\eta(E_n) = \text{sign}(E_n - E_{\text{lev}} - 0). \tag{A.13}$$

At $E_m \neq E_n$ we can write

$$\begin{aligned}
&\text{Im} \frac{1}{[\omega - E_m + i0\eta(E_m)][\omega - E_n + i0\eta(E_n)]} \\
&= -\pi\eta(E_m)\delta(\omega - E_m) \frac{1}{\omega - E_n} - \pi\eta(E_n)\delta(\omega - E_n) \frac{1}{\omega - E_m} \\
&= -\pi[\eta(E_m)\delta(\omega - E_m) - \eta(E_n)\delta(\omega - E_n)] \frac{1}{E_m - E_n}.
\end{aligned} \tag{A.14}$$

What to do in the case $E_m = E_n$ depends on whether we consider the case of infinite volume, where most of the spectrum is continuous, or whether we work in a large but finite box, in which case the spectrum is quasi-discrete. We concentrate on the latter case, since it is relevant for the numerical calculations. In the quasi-discrete case, if $E_m = E_n$ one should write instead of Eq.(A.14):

$$\text{Im} \left. \frac{1}{[\omega - E_m + i0\eta(E_m)][\omega - E_n + i0\eta(E_n)]} \right|_{E_m=E_n}$$

$$\begin{aligned}
&= \text{Im} \frac{1}{[\omega - E_m + i0\eta(E_m)]^2} = -\frac{\partial}{\partial\omega} \text{Im} \frac{1}{\omega - E_m + i0\eta(E_m)} \\
&= \frac{\partial}{\partial\omega} \pi\eta(E_m)\delta(\omega - E_m) = \pi\eta(E_m)\delta'(\omega - E_m).
\end{aligned} \tag{A.15}$$

Note that the same result would be obtained if one took the limit $E_n \rightarrow E_m$ in Eq.(A.14). We can now split the double sum over m, n in Eq.(A.12) in two parts containing, respectively, terms with $E_m \neq E_n$ and $E_m = E_n$ and perform the integral over ω using Eqs.(A.14) and (A.15). One obtains

$$\begin{aligned}
&[u(x) - d(x)]^{(1)} \\
&= (2T^3) \frac{N_c M_N}{24I} \sum_{\substack{n,m \\ E_m \neq E_n}} \frac{1}{E_n - E_m} \langle n|\tau^a|m\rangle \\
&\quad \times \langle m|\tau^a(1 + \gamma^0\gamma^3) \left\{ \eta(E_n)\delta(E_n + P^3 - xM_N) - \eta(E_m)\delta(E_m + P^3 - xM_N) \right\} |n\rangle \\
&+ (2T^3) \frac{N_c M_N}{24I} \sum_{\substack{n,m \\ E_m = E_n}} \langle n|\tau^a|m\rangle \langle m|\tau^a(1 + \gamma^0\gamma^3)\eta(E_n)\delta'(E_n + P^3 - xM_N)|n\rangle.
\end{aligned} \tag{A.16}$$

The double sum over levels in the first term here can be further simplified making use of the identity

$$\begin{aligned}
&\langle n|\tau^a|m\rangle \langle m|\tau^a(1 + \gamma^0\gamma^3)\delta(E_n + P^3 - xM_N)|n\rangle \\
&= \langle m|\tau^a|n\rangle \langle n|\tau^a(1 + \gamma^0\gamma^3)\delta(E_n + P^3 - xM_N)|m\rangle,
\end{aligned} \tag{A.17}$$

which holds for any pair of levels m, n .

Equation (A.16) pertains to a quasi-discrete spectrum; in the continuum case one should replace there the summation over levels by an integral over the continuous energy, omit the sum over terms with $E_m = E_n$ in the last line, and understand the poles $(E_n - E_m)^{-1}$ in the principal value sense.

In Eq.(A.16) the sum over n runs over all quark single-particle levels, both occupied and non-occupied. In order to convert it to a more standard form, particularly for use in the numerical calculations, we would like to rewrite the expression for the distribution function as a sum over either occupied or non-occupied states (*cf.* the standard expression for the moment of inertia, Eq.(2.14)). To achieve this we note that the following sum over *all* levels is zero:

$$\begin{aligned}
&2 \sum_{\substack{n,m \\ E_m \neq E_n}} \frac{1}{E_n - E_m} \langle n|\tau^a|m\rangle \langle m|\tau^a(1 + \gamma^0\gamma^3)\delta(E_n + P^3 - xM_N)|n\rangle \\
&+ \sum_{\substack{n,m \\ E_m = E_n}} \langle n|\tau^a|m\rangle \langle m|\tau^a(1 + \gamma^0\gamma^3)\delta'(E_n + P^3 - xM_N)|n\rangle = 0.
\end{aligned} \tag{A.18}$$

To prove this identity we note that the L.H.S. can equivalently be written as the variation of a functional trace with a particular modified Hamiltonian

$$\begin{aligned}
& \text{Im} \int \frac{d\omega}{2\pi} \int_{-\infty}^{\infty} dz^0 e^{i(\omega - x M_N) z^0} \\
& \times \frac{\partial}{\partial \Lambda^a} \text{Sp} \left[\tau^a (1 + \gamma^0 \gamma^3) \exp(i P^3 z^0) \frac{1}{\omega - H(U_c) - \Lambda^b \tau^b + i0} \right] \Big|_{\Lambda=0} \\
& = \int_{-\infty}^{\infty} dz^0 e^{-ix M_N z^0} \frac{\partial}{\partial \Lambda^a} \text{Sp} \left[\tau^a (1 + \gamma^0 \gamma^3) \exp(i P^3 z^0) \exp[i z^0 (H(U_c) + \Lambda^b \tau^b)] \right] \Big|_{\Lambda=0}.
\end{aligned} \tag{A.19}$$

Due to the locality of the modified Hamiltonian, $H(U_c) + \Lambda^b \tau^b$, we have

$$\langle \mathbf{X} | \exp(i P^3 z^0) \exp[i z^0 (H(U_c) + \Lambda^b \tau^b)] | \mathbf{X} \rangle = 0 \quad \text{if} \quad |z^3| > z^0. \tag{A.20}$$

Extrapolating Eq.(A.20) to $z^3 \rightarrow z^0$ (*cf.* the corresponding discussion in Refs.[9, 10]) we find that Eq.(A.19) is zero, which proves Eq.(A.18). Using Eq.(A.18), and keeping in mind the definition of $\eta(E_n)$, Eq.(A.13), we may now easily obtain from Eq.(A.16) a representation of the distribution function as a sum in which n runs either only over occupied states, Eq.(3.13), or non-occupied states, Eq.(3.15). We note that the equivalence of the representations of the distribution function as sums over occupied and non-occupied states is confirmed also by the numerical calculations.

When invoking the locality condition, Eq.(A.20), we have assumed that the ultraviolet regularization of the theory does not violate this property. For the regularization by Pauli–Villars subtraction, Eq.(3.21), this is indeed the case. Regularization by a cutoff, on the other hand, would violate Eq.(A.20), which amounts to violating the anticommutation relation of the quark fields at space–like separations, see the discussion in Refs.[9, 10].

References

- [1] E. Witten, Nucl. Phys. **B 223** (1983) 433.
- [2] T.H.R. Skyrme, Proc. Roy. Soc. **A 260** (1961) 127; Nucl. Phys. **31** (1962) 556.
- [3] G. Adkins, C. Nappi and E. Witten, Nucl. Phys. **B 228** (1983) 552.
- [4] D. Diakonov and M. Eides, Sov. Phys. JETP Lett. **38** (1983) 433;
A. Dhar, R. Shankar and S. Wadia, Phys. Rev. **D 31** (1984) 3256.
- [5] D. Diakonov and V. Petrov, Nucl. Phys. **B 272** (1986) 457; LNPI preprint LNPI-1153 (1986), published (in Russian) in: Hadron matter under extreme conditions, Naukova Dumka, Kiev (1986), p.192.

- [6] D. Diakonov and V. Petrov, Sov. Phys. JETP Lett. **43** (1986) 57;
D. Diakonov, V. Petrov and P. Pobylitsa, Nucl. Phys. **B 306** (1988) 809;
D. Diakonov, V. Petrov and M. Praszalowicz, Nucl. Phys. **B 323** (1989) 53.
- [7] D. Diakonov, Lectures given at the Advanced Summer School on Nonperturbative Quantum Field Physics, Peniscola, Spain, Jun. 2–6, 1997, hep-ph/9802298.
- [8] For a review, see: Ch.V. Christov *et al.*, Prog. Part. Nucl. Phys. **37** (1996) 91.
- [9] D.I. Diakonov, V.Yu. Petrov, P.V. Pobylitsa, M.V. Polyakov and C. Weiss, Nucl. Phys. **B 480** (1996) 341.
- [10] D.I. Diakonov, V.Yu. Petrov, P.V. Pobylitsa, M.V. Polyakov and C. Weiss, Phys. Rev. **D 56** (1997) 4069.
- [11] C. Weiss and K. Goeke, Bochum University preprint RUB-TPII-12/97, hep-ph/9712447.
- [12] P.V. Pobylitsa and M.V. Polyakov, Phys. Lett. **B 389** (1996) 350.
- [13] V.Yu. Petrov, P.V. Pobylitsa, M.V. Polyakov, I. Börnig, K. Goeke, and C. Weiss, Phys. Rev. **D 57** (1998) 4325.
- [14] K. Gottfried, Phys. Rev. Lett. **18** (1967) 1174.
- [15] For a recent review, see: S. Kumano, Saga University preprint SAGA-HE-97-97 and preprint DOE/ER/40561-255-INT96-19-01, hep-ph/9702367, Phys. Rep., in press.
- [16] M.V. Polyakov and C. Weiss, in: Proceedings of the 37th Cracow School of Theoretical Physics: Dynamics of Strong Interactions, Zakopane, Poland, May 30 – Jun. 10, 1997, published in: Acta Phys. Pol. **B 28** (1997) 2751.
- [17] J. Balla, M.V. Polyakov and C. Weiss, Nucl. Phys. **B 510** (1997) 327.
- [18] M. Glück, E. Reya, and A. Vogt, Z. Phys. **C 67** (1995) 433.
- [19] M. Wakamatsu and T. Kubota, hep-ph/9707500.
- [20] H. Weigel, L. Gamberg, and H. Reinhardt Phys. Lett. **B 399** (1997) 287.
- [21] F. Döring, A. Blotz, C. Schüren, T. Meissner, E. Ruiz-Arriola and K. Goeke, Nucl. Phys. **A 536** (1992) 548.
- [22] J.C. Collins and D.E. Soper, Nucl. Phys. **B 194** (1982) 445.
- [23] R.P. Feynman, in: Photon–Hadron Interactions, Benjamin, 1972.
- [24] M. Arneodo *et al.*, Phys. Rev. **D50** (1994) R1.
- [25] M. Wakamatsu, Phys. Rev. **D 46** (1992) 3762;
A. Blotz, M. Praszalowicz and K. Goeke, Phys. Rev. **D 53** (1996) 551.

- [26] H. Walliser and G. Holzwarth, Phys. Lett. **B 302** (1993) 377.
- [27] S. Kahana and G. Ripka, Nucl. Phys. **A 429** (1984) 462.
- [28] M. Wakamatsu and H. Yoshiki, Nucl. Phys. **A 524** (1991) 561.

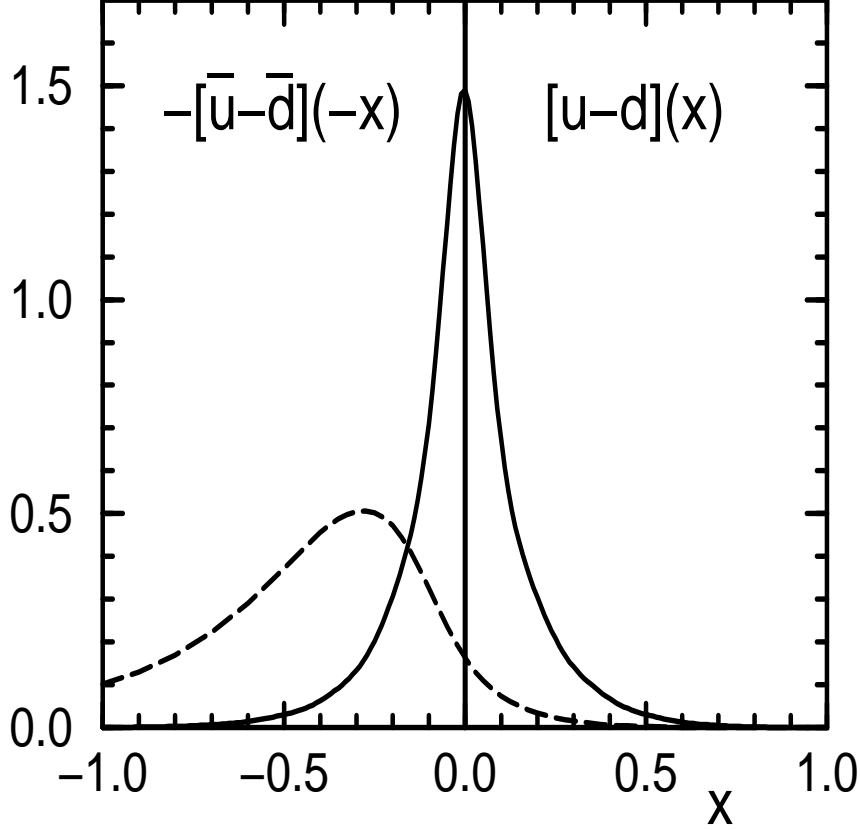


Figure 1: The contribution of the Dirac continuum to the isovector distribution function $u(x) - d(x)$, for $M = 350 \text{ MeV}$. At negative x the function shown describes minus the antiquark distribution. *Solid line*: Total result, as obtained from the expansion in angular velocity, given by the sum of Eq.(3.18) and Eq.(3.19). *Dashed line*: Result obtained dropping the contribution Eq.(3.19), corresponding to the prescription of Ref.[19].

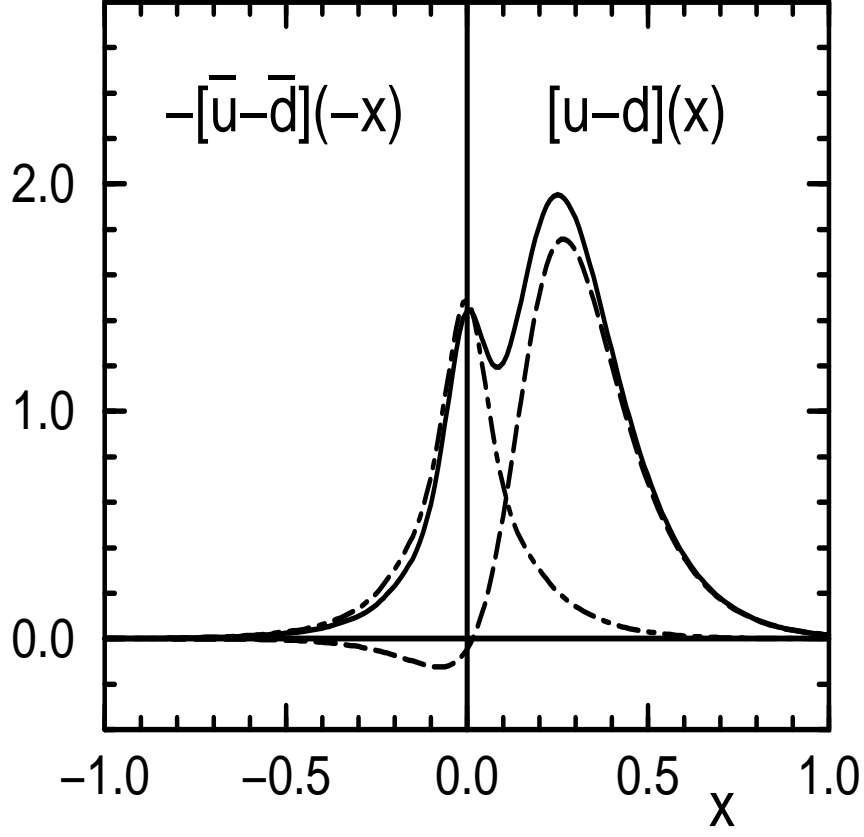


Figure 2: Contributions to the isovector unpolarized distribution function, $u(x) - d(x)$, for $M = 350$ MeV. At negative x the function shown describes minus the antiquark distribution. *Dashed line*: Contribution of the discrete level. *Dot-dashed line*: Contribution of the negative Dirac continuum. *Solid line*: Total result.

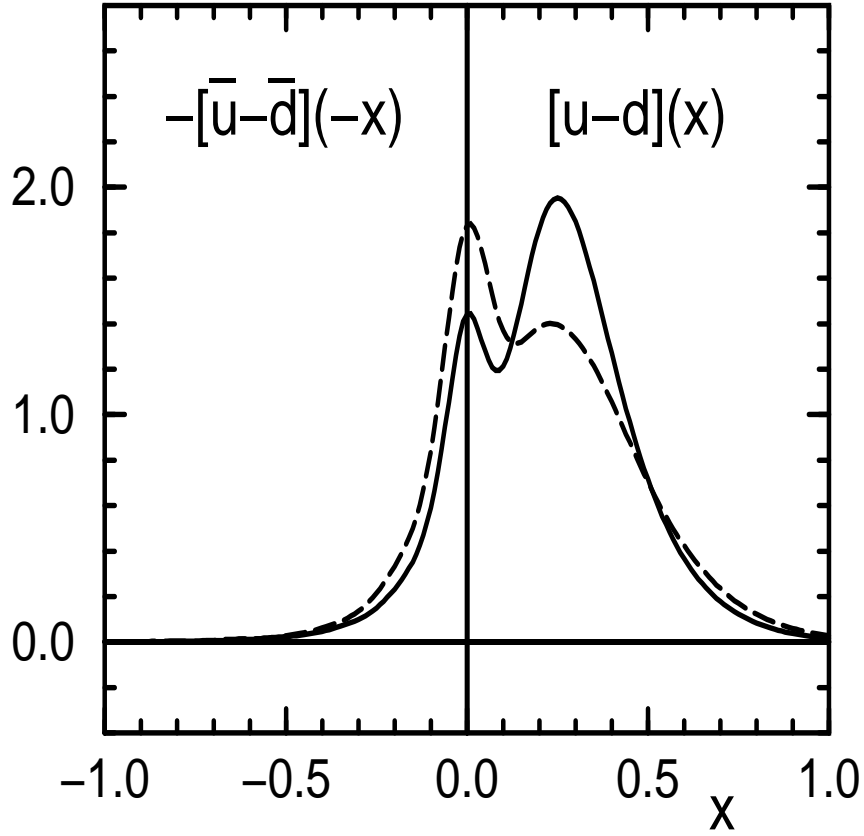


Figure 3: The isovector unpolarized distribution function, $u(x) - d(x)$, for constituent quark masses $M = 350$ MeV (*solid line*) and $M = 420$ MeV (*dashed line*). At negative x the function shown describes minus the antiquark distribution.

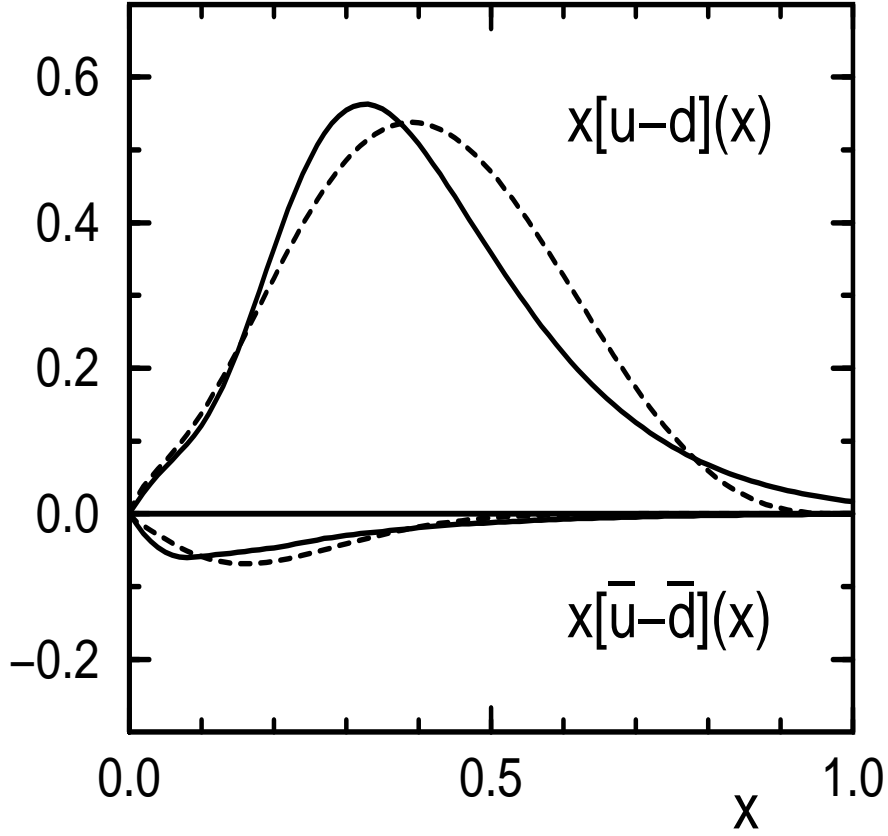


Figure 4: *Solid lines:* The calculated isovector unpolarized quark- and antiquark distributions, $x[u(x) - d(x)]$ and $x[\bar{u}(x) - \bar{d}(x)]$, for $M = 350$ MeV. Shown is the total result, corresponding to the solid line in Fig.2. *Dotted lines:* The GRV NLO parametrizations [18].